Investigation of the effectiveness of PCM on the energy saving, thermal comfort and indoor air quality in overcrowded area

Fadhil A. M. K. Al-Malaki[a], Hasanen M. Hussen[b], Göker Türkakar[c], Rahim Jafari[d,*]

[a] Department of Mechanical Engineering, Atilim University, Ankara, Türkiye
[b] Mechanical Engineering Department, University of Technology-Iraq, Baghdad, Iraq
[c]Department of Mechanical Engineering, Zoguldak Bulent Ecevit University, Zonguldak, Türkiye
[d]Department of Automotive Engineering, Atilim University, Ankara, Türkiye

Keywords: Phase change material, PCM, energy consumption, thermal comfort

Abstract

Overcrowded areas like hospitals, jails, and shelter elevators pose a risk in terms of excessive temperatures, excessive CO_2 concentrations, or even the presence of toxins and viruses. Hence, ventilation, thermal comfort and energy management are crucial issues for these kinds of places. In the present study, a prototype (1:4) of a prison quarry located in Baghdad, Iraq has been examined. Indoor air quality, humidity, temperature distribution and energy consumption of the room have been monitored for the identical weather conditions of the real prison cell, including five dummy occupants, each dissipating 100 W/m^2 of heat, releasing CO_2 of 0.3 l/min and water vapor. To reduce the cooling energy consumption of the building and the temperature deviation during the day, two layers of Phase Change Materials, PCMs, have been embedded in the ceiling of the prototype. Experiments have been recorded for three hours in Baghdad's harsh weather conditions in August. In addition, numerical analyses were conducted and compared with experimental findings, and a good match is obtained. Energy saving of 47.2% have been calculated by using PCM for the inlet air velocity of 0.5 m/s.

* Corresponding author
Email address: rahim.jafari@atilim.edu.tr
Address: Kizilcasar street, incek,06830, Ankara, Türkiye

Nomenclature

C_p	: specific heat [J kg^{-1} K^{-1}]	**Greek Let.**	
f	: melt fraction	α	: diffusivity [m^2/s]
F	: body force per unit volume [N m^{-3}]	ρ	: density [kg/m^3]
k	: thermal conductivity [W m^{-1} K^{-1}]	μ	dynamic viscosity [N·s m^{-2}]
L	: latent heat of fusion [J kg^{-1}]	**Subscripts**	
h	: enthalpy [kj kg^{-1}]	i	: inner
h	: heat tr. coef. [W m^{-2} K^{-1}]	l	: liquid
H	: total enthalpy [J m^{-3}]	o	: outer
P	: pressure [Pa]	s	: solid, sensible
$\vec{q}$	: heat flux vector [W m^{-2}]	**Abbreviations**	
T	: temperature [K]	Al	: aluminum
u	: velocity [m s^{-1}]	PCM	: Phase Change Material
x_m	: solid liquid interface position	Rad	: radiation

1. Introduction

Thermal energy storage (TES) is a key advanced renewable technology that has been increasing interest in its use for heating and cooling applications in buildings in recent years [1]. The capability of Phase Change Materials (PCMs) to absorb, store and release of thermal energy in the form of latent heat during the phase change makes them to be considered as a promising TES material [2,3][2,3]. It causes the cooling load to shift from peak to off-peak hours and improve system efficiency by lowering the needed capacity [4] and chiller partial-load operations [5].

In this context, various studies have been conducted [6,7] and incorporating PCMs with building walls [8], roof [9], concrete [10], window shutter [11], insulations [12] and bricks [13] have been investigated.

Prabhakar et al. simulated office buildings containing PCM in different climate conditions. By combining a PCM passive system with night ventilation, the efficacy of PCM was raised from 3.32% to 25.62% in temperate conditions. When PCM was combined with temperature-controlled airflow, the improvement increased to 40%. It was discovered that using only PCM as a passive

cooling device in workplace buildings during cooling months was ineffective in hot and dry climate conditions [14].

In the extremely hot climate of Al Amarah city, Iraq, Al-Yasiri and Szabo investigated two identical rooms, one its walls and ceiling loaded with PCM and the other without (the reference room). It was determined that, in comparison to the reference room, the PCM significantly improved the thermal efficiency of the PCM room during the hot hours. Additionally, the PCM room's ceiling performed thermally better than the walls [15]. The average heat and associated CO_2 emission reductions were reported 56 W and 1.35 kg/day, respectively [16]. They also investigated the thermal performance of a room containing PCM based on the effectiveness of the natural night ventilation period on the thermal performance of a room-integrated PCM. The increase in the natural night ventilation time from 1 to 4 hours reduced the average indoor air temperature by 28.6% during the day. Although the period affected the temperature, the results showed that the average heat gain difference did not change considerably in the next day-cycle [17].

Golamibozanjani and Farid modeled an active air-PCM heat exchanger two-dimensionally. The natural convection inside the molten layer, thermal mass of the metal heat exchanger and volume expansion of PCM were taken into account [18]. In addition, they compared the thermal performance of active and passive PCM systems experimentally. Considering the space cooling scenario, the active PCM system consumed slightly higher energy than the passive PCM system. On the other hand, the active PCM system consumed 22% less energy comparing the passive PCM system for space heating [19].

Bohorquez- Ordenes et al. carried out thermal simulations of a house with variable thickness of PCM layers. Reduction in the thermal discomfort hours increased for both passive and active analyses as the thickness of the PCM layer varied from 2 mm to 10 mm. Besides, the total electricity consumption for the cooling demand fell by 60.3% by using the PCM layer [20].

Hagenau and Jradi simulated a standard Danish office to select the optimal PCM from examined 17 PCMs. It’s been concluded that a PCM with a melting temperature of 24 °C, latent heat of fusion of 219 kJ/kg, and a crystallization temperature of 21 °C had the best performance. In addition, based on the parametric analysis, it was resulted that the best energy performance and

indoor thermal comfort were obtained by using of 40 mm PCM layer on the interior side of the building components [21].

Ma at el. investigated the temperature and energy consumption of a rural residential building containing a sunspace in a sever cold area. It's been concluded that the heating energy consumption by using PCM and PCM+Silica aerogel glass were reduced by 10% and 14%, respectively compared to the reference sunspace with a hollow to the building [22].

Yang et al. numerically evaluated the performance of encapsulated PCM ceiling panels. The findings show that the panel made of a pyramid array performs better thermally than the tetrahedral-based one and for the panel volume of 250 mL, the average melting rate is 20.8% higher. In addition, the heat transfer performance is enhanced by hanging the panel instead of attaching it to the ceiling [23].

Rangel et al. evaluated the thermal performance in a chamber considering the effect of PCM and natural convection for semi-arid climatic conditions, experimentally. The best results were achieved when PCM was combined with a 30 cm air gap without natural ventilation. It lowered the internal air temperature by 2.5 °C. Besides, it resulted in a lag time of 70 min [24].

Nemeth et al. examined two model houses, one as a reference and the other one equipped with plaster lining containing incorporated PCM microcapsules. The experiments were conducted during the winter by heating daytimes and cooling in the nights. The results revealed that the PCM improved the thermal performance by increasing the inner walls temperatures, typically from 23 °C to 27 °C, and reducing the power demand of electric radiator by 10.3%. The inner walls temperatures and the energy demand reduced to 25 °C and 7%, respectively by applying heat pumps instead of electric radiator [25].

Mousavi et al. experimented full-scale cabin equipped with phase change material embedded radiant chilled ceiling. Aim was to improve energy efficiency and indoor environmental quality, and also provide demand-side flexibility. The electricity demand was met mostly (80% of the total use) during off-peak hours. Class B thermal comfort according to ISO7730 standards is obtained [26].

Alassaad et al. conducted laboratory experiments to determine the PCM integrated lightweight earth based material. Earth-based material-PCM mix material is mounted on the exterior walls of

family houses on Caen and Nice, France. As a result of the simulations, energy savings of heating/cooling requirements are achieved at 62% in Caen, and 67% in Nice [27].

Sub-scaled experimentation for cooling/heating applications for buildings is widespread in the literature. Zhu et al [28] experimentally investigated two reduced-scale test chambers, one coated with microencapsulated PCM. Under 80 W/m^2 heating load, while the PCM coated chamber could maintain the room temperature between 26-28°C for 77 mins, the other room could maintain that temperature level for only 13 mins. Similarly, Berardi and Soudian [29] replicate typical apartment units with 1:10 scale. 2 layer PCMs (with melting temperatures of 21.7 and 25°C) are applied to the walls of the test chamber. They observed that peak temperature is reduced up to 6°C in the room equipped with PCMs. Besides, it prevented sharp temperature fluctuations in the room even in strong outdoor environmental changes. Many studies in the literature studying in this field used subscale chambers in their experimental work [30-33] because of reasons like; cost, setup manageability, size of the lab area, and time constraints [33].

Recent studies related to peak electricity shaving, energy saving and indoor thermal condition are listed in Table 1.

Table 1 Recent studies related to peak electricity shaving, energy saving and indoor thermal condition

Author/ year	Geometry/ Location	Methodology	Energy Storage Material	Remarks
Prabhakar et al. [14], 2020	Office building, 15 different city.	Simulation-based optimization. EnergyPlus software.	RT24	The effectiveness of the PCM was raised from 3.32% to 25.62% by a combination of PCM and nighttime ventilation.
Al-Yasiri and Szabo [17], 2022	Al Amarah, Iraq.	Experimented two identical rooms. One with PCM (roof and walls).	Paraffin wax, 40-44°C	A remarkable benefit of PCM has been observed for 6 hours of natural night ventilation.
Gohar Gholamibozanjani, et al. [19], 2020	Two cabins are built, New Zealand	Huts are experimentally compared regarding passive or active cooling strategies.	Passive conf (PT20), active conf. (RT25HC).	As a result of 10 days experiment in winter, the energy consumption of the hut with active cooling was 22% less.
Bohorquez-Ordenes et al. [20], 2021	A house in Chile	Numerical simulations	InfiniteRPCM2 3C, 22-24°C	Thermal discomfort hours have been reduced by 25.43% with a 10 mm thick PCM layer. Total energy consumption was 60.3% lower than the house without PCM layers.
Hagenau and Jradi [21], 2020	A Danish office, in Denmark	Simulations with EnergyPlus	Investigated 17 PCMs	PCM melting at 24°C with latentheat of 219 kJ/kg performed the best. 40 mm PCM layer at the interior yielded the best scenario.
Ma et al. [22], 2023	A rural residential building heating with sunscreen, China.	Simulations with EnergyPlus	PCM(cetane paraffin) and PCMs Silica aerogel	Energy consumption has been reduced 10% and 14% with the application of PCMS and PCMS-silica compared to without PCM use, respectively.
Nameth et al. [25], 2023	Bácsalmás, southern Hungary, two model houses.	Experimental, 2 consecutive winters	PCM (RT25) plaster lining	PCM plaster lining equipped house consumed 10.7% and 7% less energy than the standard house heated by an electric heater and heat pump, respectively.
Mousavi et al. [26], 2023	Test cabin, Melbourne.	Experimental.	PCM-Radiant Chlled Ceiling Incorporating	4-5 h overnight chilled water circulation was enough for a fully recharge. 70% of the total electricity use was concentrated during off-peak hours.
Alassaad et al. [27], 2023	A typical family house, in France (Nice and Caen)	Experimental (to determine the material properties), Numerical.	PCM (LE0 and LE20) within the lightweight earth-based material.	Energy savings have reached 62% in Caen, and 67% in Nice regarding heating/cooling requirements.

When considering the significant energy consumption of the buildings and its transient behavior, at the same time, maintaining indoor environment quality requires a smart control mechanism. Elnour et al. a neural network-based model predictive control management and optimization system is generated for the HVAC system of a building [34]. Artificial intelligence and big data are other research subjects for building automation and management systems [35,36]. Simulation-based approaches, artificial intelligence, machine learning, and optimization algorithms are the alternative energy management strategy approaches [37]. On a larger scale, creating smart cities targeting net zero emissions, low waste energy, and relatively stable grid is the ultimate aim. To be able to do this, artificial intelligence, the Internet of Things, and communication technologies are employed to gather and analyze big data [38].

Although extensive studies have been conducted on PCM-based thermal storage in buildings, the majority of research has investigated just the effect of the PCMs on the overall temperature and energy consumption. However, further research is required to investigate their effects on indoor air quality (IAQ) which includes airflow, management of organic volatile compounds, air temperature distribution, CO_2 dispersion, and relative humidity inside the buildings. In addition, overcrowded areas like hospitals, jails, and shelter elevators pose a risk in terms of excessive temperatures, excessive CO_2 concentrations, or even the presence of toxins and viruses. Hence, the investigation of the effectiveness of PCMs on the aforementioned parameters seems crucial.

It is not completely fair to compare the studies in the literature regarding their energy-saving rate as the operating conditions are not the same. However, it is important to understand in terms of how impactful the PCM is. Among the recent studies of the literature, Bohorquez- Ordenes et al. [20] and Alassaad et al. [27] have reached the best energy-saving rates as a result of their simulations with 60.3 and 67%, respectively. On the other hand, 47% maximum energy saving has been reached in the present study. In addition to the energy-saving ratio, the present study also examines the IAQ, CO_2 dispersion, and relative humidity of the building.

In the present study, a prototype of a prison quarry located in Baghdad, Iraq with dry and hot weather in summer days has been examined. Five dummy occupants were considered in various positions, each dissipating heat, releasing CO_2 and water vapor. The prototype includes two layers of PCMs embedded in the ceiling and was compared with the reference one. Additionally,

comprehensive transient Computational Fluid Dynamics analyses were conducted to monitor the temperature distribution, CO_2 level, humidity, and energy consumption for various inlet air velocities.

2. Material and Methods

This section is divided into two main subsections. Firstly, the experimental test setup is explained. Afterward, the numerical model to simulate two rooms containing dummy occupants with and without PCMs embedded in the ceiling are described.

2.1. Experimental test setup

This section is comprised of four parts including test setup description, measurements, PCM characterization, and uncertainty analysis.

2.1.1. Experimental test setup geometry

The prototype model (1/4 scaling) used in this study is based on a real prison cell with dimensions of 4800 mm in length (1200 mm for the model), 2400 mm in width (600 mm for the model), and 3200 mm in height (800 mm for the model). It is considered that five people accommodate in the cell. The human body was represented as a cylinder with a cap, with dimensions of 30 mm in diameter and 400 mm in height. Two dummy cylinders representing two people are positioned horizontally. The rest are positioned vertically as shown in Fig. 1. A heating pad inside the cylinders provides 100 W/m^2 heat flux representing an individual's heat dissipation to its surrounding. The room has no windows and no openings to the outside. The walls of the experimental model were constructed of insulated Perspex sheets with a thickness of 6 mm, which were attached to the steel structure of the model using studs. The supply and return grilles were the only connection between the room and the outside world. While the inlet grill was positioned on the western wall and had dimensions of 80 mm × 60 mm with a 60 mm distance to the ceiling, the exhaust grill with dimensions of 100 mm × 80 mm is positioned 50 mm above the eastern wall. An air conditioning laboratory unit was used to control the inlet temperature and velocity.

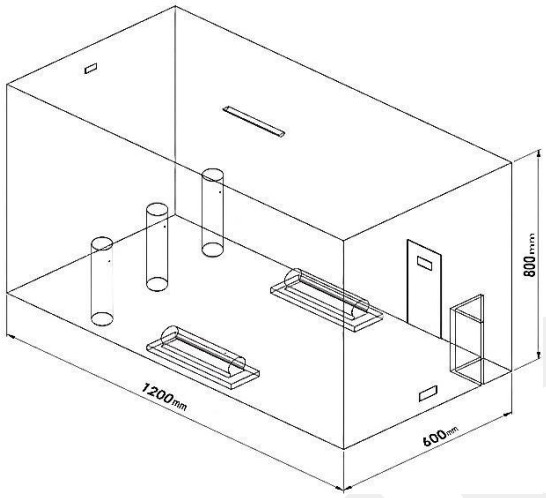

Figure 1 Test setup geometry

The ceiling of the experimental apparatus was made of an aluminum container filled with PCMs. Two identical aluminum containers were used, each containing a different PCMs with dimensions of 1200 mm × 600 mm × 25 mm as shown in Fig.2.

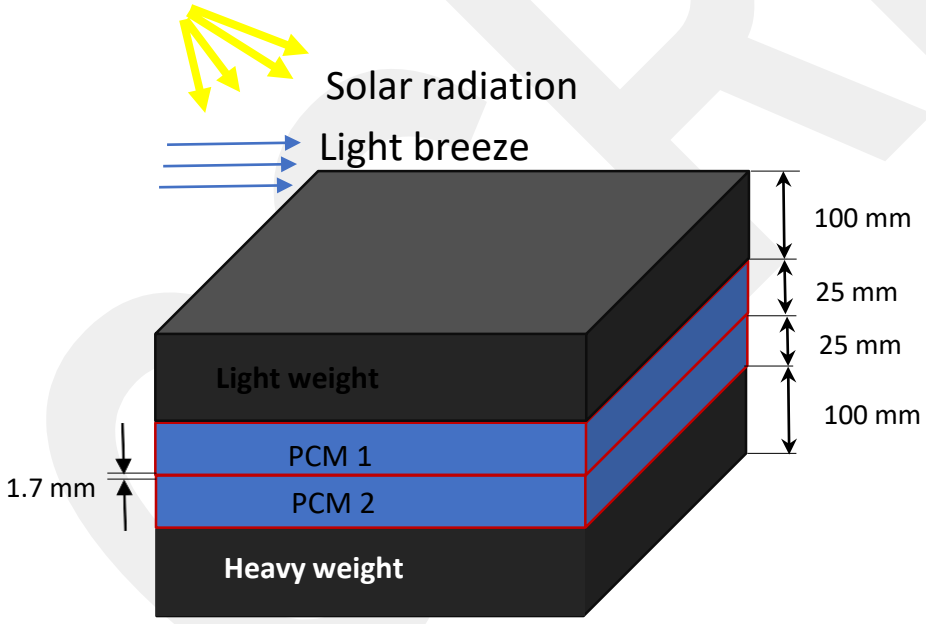

Figure 2 Ceiling configuration with embedded PCMs

A sober inhalation and exhalation system for the pseudo dummy was created. It consists of solenoid valves, a two-way pump, a CO_2 gas bottle, a fitting segmentation, and a tube orifice grid. The system is controlled by Arduino.

2.1.2. Experimental measurements

The indoor monitoring system developed in this study utilizes a system architecture with sensor nodes that measure primary variables such as temperature, humidity, air velocity, and CO_2 concentration. These sensor nodes are managed by two Arduino microcontrollers. The recorded information is transferred to a PC for display. Figure 3 depicts the test setup. The indoor air speed, relative humidity, CO_2 concentration, and indoor air temperature are measured using a digital-output relative humidity sensor (model DHT22) for temperature and humidity, an MG-811 GAS SENSOR, and an MQ-2 GAS SENSOR for CO_2 concentration, and a hot wire anemometer (model Lutron YK-2005AH) for the air velocity. Detailed information can be found in [39].

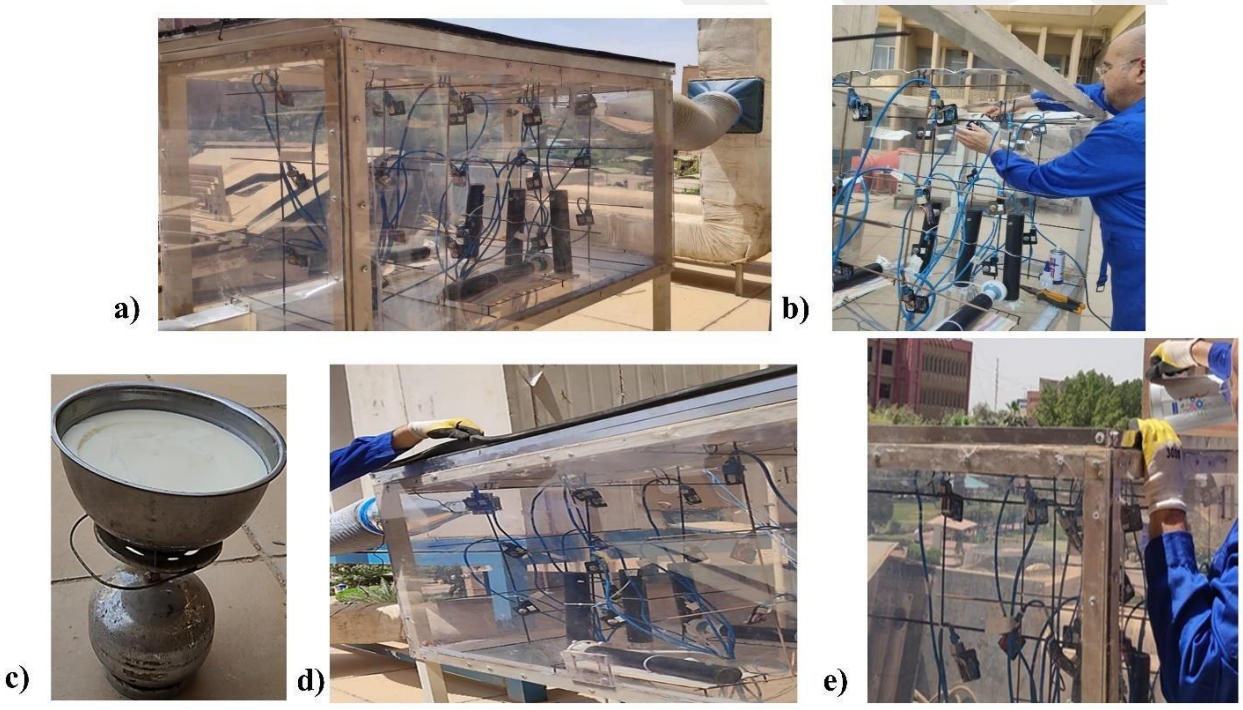

Figure 3 Test setup, a) complete portotype model prior to insulation, b) setup installation, c) PCM melting, d) PCM placement stage, e) PCM puring to the top

2.1.3. Characterization of PCMs

Two different compositions of local paraffin waxes, named as PCM_1 and PCM_2, have melting points suitable for Iraq's hot and cold conditions, respectively. They are made of a mixture of soft wax (20 % for PCM_1 and 100 % for PCM_2) and crystal wax (80 % for PCM_1). These PCM_s were used in roof construction. Differential Scanning Calorimeters (DSC) analysis has been carried out

to determine the melting range and heat storage ability of the PCMs. The main thermophysical properties are provided in Table 2.

Table 2 PCMs properties

Parameter	Unit	Value	
		Paraffin's Wax	
		PCM_1 (RRM1)	PCM_2 (RRM2)
Melting point	˚C	40-55	19-37
Density (ρ_s)	(kg/m^3)	1270	785
Density (ρ_l)	(kg/m^3)	1180	749
Specific Heat (C_p) at solid	(kJ/kg ˚C)	2.71	1.4
Specific Heat (C_p) at liquid	(kJ/kg ˚C)	2.87	2.2
Thermal Conductivity (k_s)	(W/m K)	0.41	1.09
Thermal Conductivity (k_l)	(W/m K)	0.22	0.51
Diffusivity α_s	(m^2/s)	2.6×10^{-4}	9.9×10^{-5}
Diffusivity α_L	(m^2/s)	1.0×10^{-4}	3.03×10^{-5}
Layer thickness	cm	2.5	2.5
Enthalpy (h)	(kJ/kg)	250	146

2.1.4. Uncertainty analysis

Uncertainties of the measuring devices are summarized in Table 3.

Table 3 Uncertainty values

Parameter	Measuring device	Model	Uncertainty Value	Units
Mean temperature in PCM_s	Thermocouple	Type (K)	±1.2	˚C
Indoor air temperature	Digital-output	DHT22	±0.5	˚C
Air relative humidity	Digital-output	DHT22	±0.2%	RH
Air velocity	Anemometer	No. yk-2005AH	±0.025	m/s
CO_2 concentration	Gas sensor	MQ-135 GAS	±1.0	ppm
CO_2 concentration	Gas sensor	Mg-811 GAS	±1.0	ppm

Breathing airflow	Hot wire Anemometer	No. yk-2005AH	± 0.01	m^3/s

2.2. Numerical Model

2.2.1. Geometry and computational domain

The geometry of the numerical model is exactly the same as the scaled room constructed for the experimentation. Five dummy occupants with the same dimensions and positions as in the experimental setup are considered for the simulation. Each body generates heat flux of 100 W/m^2. A fluorescent light with a power consumption of 10 W with no open exposure due to security concerns was simulated by constant power generation. A carbon dioxide rate of 0.3 l/min is considered to be emitted from the mouth of the dummy body [40]. ASHRAE Standard recommends that the temperature and humidity of exhaled air are 33 °C and 95 %, respectively [41].

The setup is sub-scaled with 1/4 ratio. As the sizes shrink, the heat load, the air's mass flow rate, the setup's surface area, PCM mass, and human model sizes are reduced in the same order. Therefore, a similarity between the real size model can be obtained. If the natural convection were dominant in the cabin, size would matter. However, there is forced convection inside the room with the same inlet Re numbers. Hence the heat transfer behavior between the surfaces and fluid is expected to be similar. As a result, it is expected there is no major reason for deviation between the scaled model and the real size case. The important parameters like energy saving, temperature distribution, and PCM melting characteristics are not significantly affected by scaling. In addition, the main aim of the present study is the comparison between the room with PCM and the one without PCM. Subscaled studies are widespread in the literature as mentioned in the introduction section and the same procedure, which has been used in this study have been employed [29-33].

2.2.2. Governing equations

Continuity, momentum, and energy equations are solved for the room and the PCM regions. Transient analysis on the room region has been performed under the assumptions of three-dimensional geometry, incompressible, k-ε turbulent flow. Three-hour analysis is performed

starting at 12 PM to 15 PM for Baghdad, Iraq's conditions in August. The continuity equation is given in Eq. 1 as

$$\frac{\partial \rho}{\partial t} + \nabla \cdot (\rho \vec{u}) = 0 \quad (1)$$

$\vec{u}$ is the three-dimensional velocity vector. The momentum equation for constant viscosity is provided in Eq. 2

$$\rho \frac{\partial \vec{u}}{\partial t} + \rho(\vec{u} \cdot \nabla)\vec{u} = -\nabla P + \mu \nabla^2 \vec{u} + + \vec{F} \quad (2)$$

$\vec{F}$ in Eq. 2 is the body force per unit volume. The energy equation neglecting the viscous dissipation for the air region is provided in Eq. 3 as

$$\rho_p C_p \frac{\partial T}{\partial t} + \rho_p C_p (\vec{u} \cdot \nabla)T = k \nabla^2 T \quad (3)$$

The inlet air temperature is 16 ℃. The air in the room is in thermal interaction with the PCMs at the top. The air inlet velocity varies for different cases (0.5, 1, and 2 m/s). All walls are thermally insulated. The ceiling is also considered insulated for cases without PCMs. A three-hour transient analysis starting from 12 PM to 15 PM has been carried out.

Thermophysical properties of the construction materials of the room are provided in Table 4.

Table 4 Material properties of the simulated room

Part	Material Type	Density (ρ) kg/m^3	Specific Heat (C_p) J/(kg·K)	Thermal Conductivity (k) W/(m·K)
Ceiling	Aluminum	2719	871	202.5
Floor and Insulators	Glass-Wool	64	670	0.04
Side Walls	Perspex	1180	1450	0.2

It is presumed that there is no natural convection in the PCMs. In addition, PCM properties are constant for the solid and liquid phases, the only heat transfer mechanism is the thermal conduction in one dimension. At the initial state, the PCMs are completely solid, and their temperatures are at 16 °C. The general energy equation in the PCM regions is given in Eq. 4 as [42]

$$\frac{\partial H}{\partial t} + \nabla(\vec{u} H) = -\nabla \cdot \vec{q} \tag{4}$$

H in Eq. 4 represents the total enthalpy, $\vec{u}$ is the liquid phase PCM velocity (neglected), $\vec{q}$ is the heat flux vector.

$$H(T) = \Delta H(T) + h_s(T) \tag{5}$$

$$\Delta H(T) = \rho\, f(T)\, L_{FDM} \tag{6}$$

f in Eq. 6 is the melt fraction, h_s is the enthalpy value of the PCM which can be calculated using Eq.7 as [43]

$$h_s = h_{ref} + \int_{T_{ref}}^{T} \rho_{PCM}\, C_{PCM}\, dT \tag{7}$$

$$f = \begin{cases} 0, & T < T_s \\ ]0,1[, & T_s < T < T_l \\ 1, & T > T_l \end{cases} \tag{8}$$

The first term in Eq. 7 is the reference enthalpy. Liquid fraction gets the value of zero if it is below the solidus. Its value is 1 if the PCM is above the liquidus temperature. If Eq. 7 is expressed in terms of h_s by neglecting the liquid PCM motion,

$$\frac{\partial h_s}{\partial t} = -\nabla \cdot \vec{q} - \rho_{PCM}\, L \frac{\partial f}{\partial t} \tag{9}$$

Solid-liquid interface is determined by Stefan condition

$$\rho_{PCM}\, L \frac{\partial x_m(t)}{\partial t} = -k_l \left(\frac{\partial T_l}{\partial y}\right) + k_s \left(\frac{\partial T_s}{\partial y}\right) \tag{10}$$

x_m is the time-dependent solid-liquid interface position. The coordinates of the PCM region are defined in Fig. 4.

Figure 4 also depicts the measured temperature values of the thermocouples. Six thermocouples were regularly embedded at the bottom, middle, and sides of the PCM panels to measure the

temperatures at six points, allowing for the prediction of the behavior of the paraffin inside the panels.

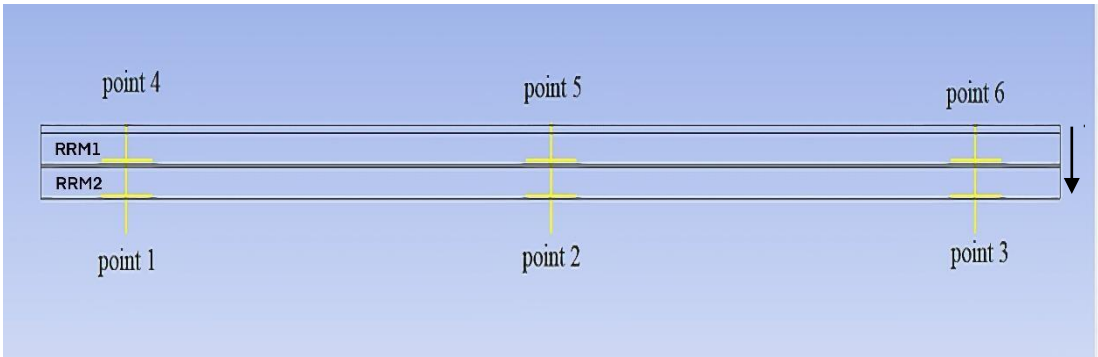

Figure 4 PCMs positions and locations of the embedded thermocouples

Ceiling of the room facing to the sky (y=0) is exposed to the thermal radiation and convection. The boundary condition for the upper PCM is given in Eq. 11 as

$$k_{PCM1}\left.\frac{\partial T}{\partial y}\right|_{y=0} = q_{rad} + h_o(T_\infty - T_{y=0}) \quad (11)$$

h_o is the heat transfer coefficient of the outside. q_{rad} is the net thermal radiation exposed to the surface at y=0. The simulations have been carried out considering the experimentation, which was conducted between 12:00 pm - 3:00 pm. The radiation at this time interval is interpolated for hourly measured as 780, 1099, 866, and 601 W/m^2, respectively. The boundary condition for the ceiling facing the interior of the room is related to the inner side convection heat transfer as

$$k_{PCM2}\left.\frac{\partial T_2}{\partial y}\right|_{y=L} = h_i(T_{y=L} - T_{room}) \quad (12)$$

The governing energy equation for the aluminum slabs is provided in Eq. 13 as

$$k_{Al}\frac{\partial^2 T_{Al}}{\partial y^2} = \rho_{Al} C_{Al}\frac{\partial T_{Al}}{\partial t} \quad (13)$$

2.2.3. Meshing of the computational domain

An unstructured tetrahedron mesh structure has been implemented. The simulations are performed with three different grid sizes of 1,004,378 1,547,700 and 2,496,452 for the inlet velocity of 0.5

m/s. The grid sizes are restricted based on the computer Ram capacity and the computational time. When a coarse mesh of 1,547,700 elements is employed, The maximum change in the air temperature and CO_2 were respectively 0.5 °C and 1.1% for the last two coarse and fine meshes, which are within the uncertainty range of measurement devices in the experimentations. Air temperature and CO_2 concentrations for coarse and fine meshes are tabulated in Table 5.

Table 5 Average air temperature and CO_2 concentrations for different mesh sizes

Type of mesh	Number of elements	Skewness	Air temperature °C	Relative difference, %	CO_2 concentration, ppm	Relative diff., %
Coarser	**1.004.378**	**0.231**	**24.2**		**729**	
Coarse	1.547.700	0.208	26.1	7.2	751	2.9
Fine	2.496.452	0.205	26.6	1.8	760	1.1

3. Results and Discussion

The numerical results are provided as contour plots from two different cross-sections. These are depicted in Fig. 5.

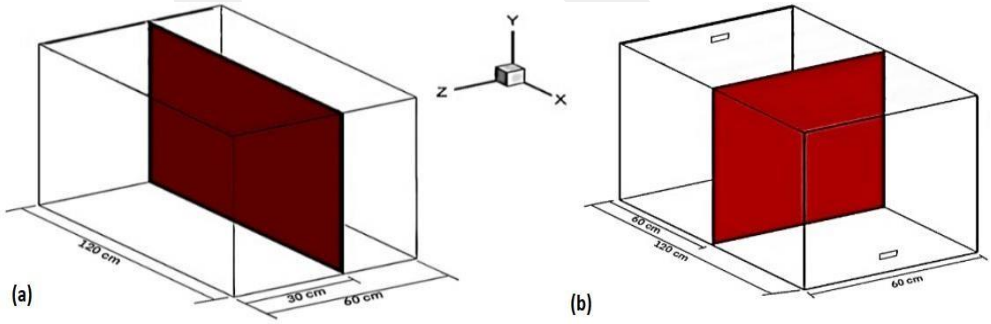

Figure 5 Cross-sectional planes (a) at Z=0.3 m and (b) at X=0.6 m for displaying the numerical results

PCM effect on the temperature pattern is investigated for the inlet air velocity of 0.5 m/s under a typical August day in Iraq. Due to restrictions to provide carbon dioxide and vapor continuously, experiments were just recorded from 12:00 pm to 3:00 pm with a peak ambient temperature of 55 °C. Solar radiation and ambient temperature data are provided in [39]. Temperature distribution of

the room with and without PCM at the moment when the cooling load peaks at 1:22 pm is shown in Fig. 6.

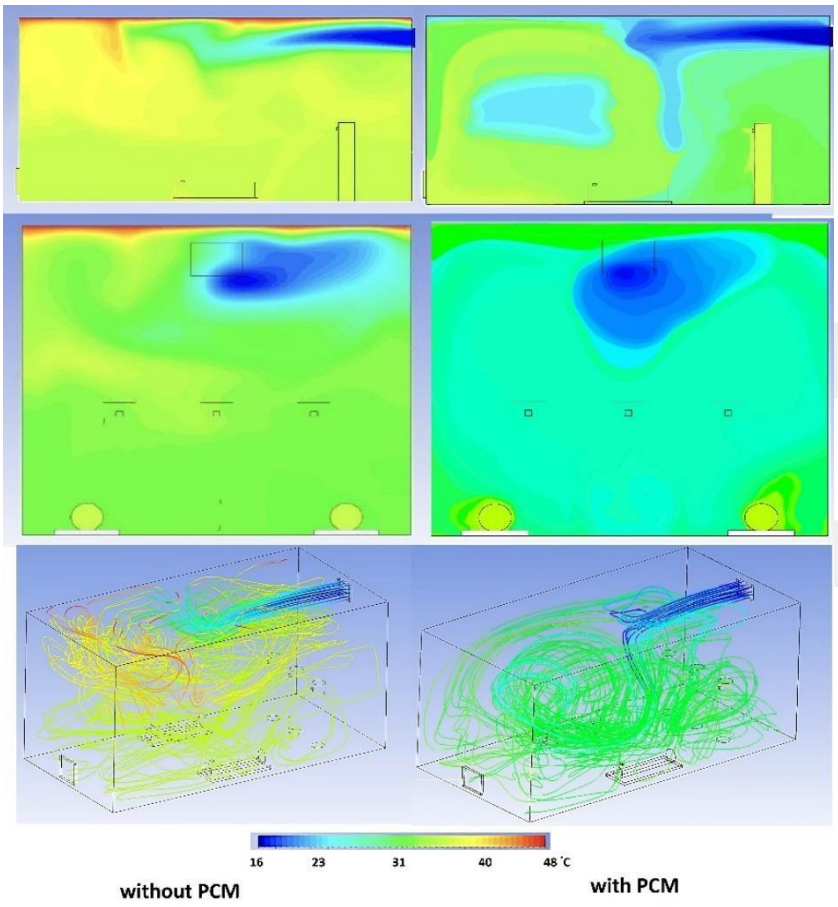

Figure 6 Temperature distributions at planes of Z=0.3 m, X=0.6 m and streamlines for inlet velocity of 0.5 m/s

It is evident that the use of PCM was beneficial in providing homogenous temperature distribution and reducing the average temperature level of the room. The temperature of the ceiling reduces to 33 °C while it remains 48 °C without PCM. In addition, the temperature at the center of the room is diminished from 35°C to 26°C by using PCM. The vortices' intensity is stronger for the room without PCM when the temperature streamlines are examined. Temperature streamlines show that PCM provides more uniform temperature distribution inside the room.

The other critical parameter for the IAQ of the room is CO_2 concentration. Figures 7 shows exhaled carbon dioxide distribution with and without PCM usage at the ceiling. In this case, carbon dioxide concentration is slightly higher without using PCM, especially in the corners in contact with lying

occupants, reaching 850 ppm due to occupants' breathing and temperature differences between zones. However, all the values remain within safe limits due to good air circulation within the space.

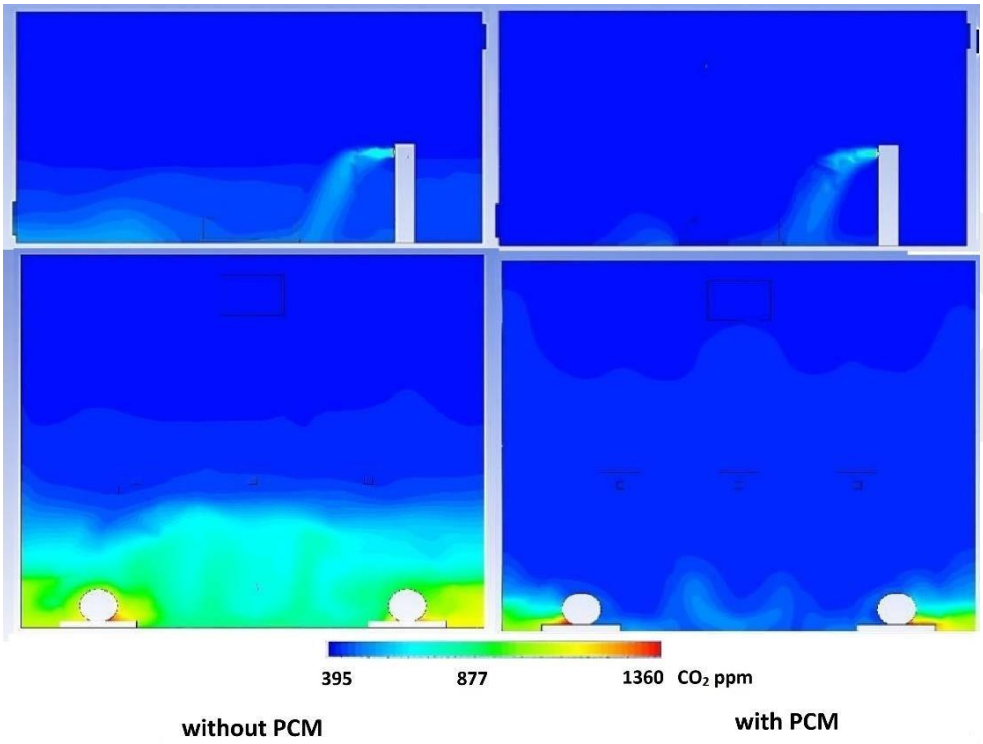

Figure 7 CO_2 concentration for inlet air velocity of 0.5 m/s with and without PCM

The effect of PCM on the distribution of exhaled vapor is illustrated as vapor volume fraction in Fig. 8. Analysis of the vapor volume fraction depicts that there is no considerable difference between the vapor volume fractions with and without PCM cases inside the room except the region near the ceiling that experiences higher values without PCM. The reason would be that the ceiling for the case without PCM experiences higher temperature than that one with PCM.

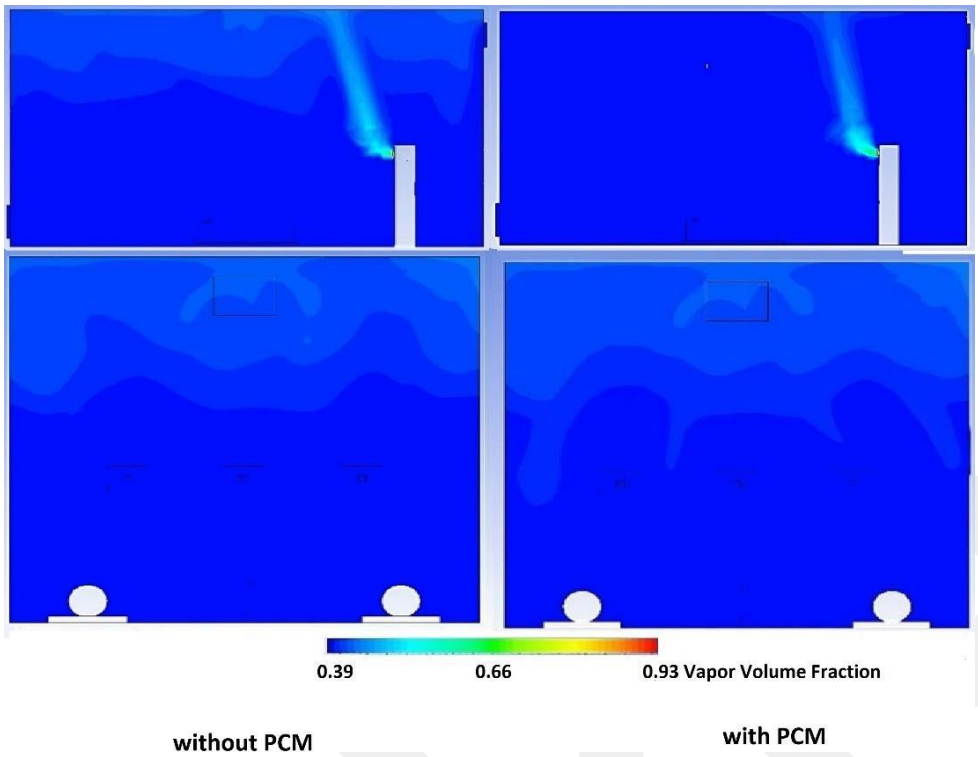

Figure 8 Vapor volume fraction for inlet air velocity of 0.5 m/s with and without PCM

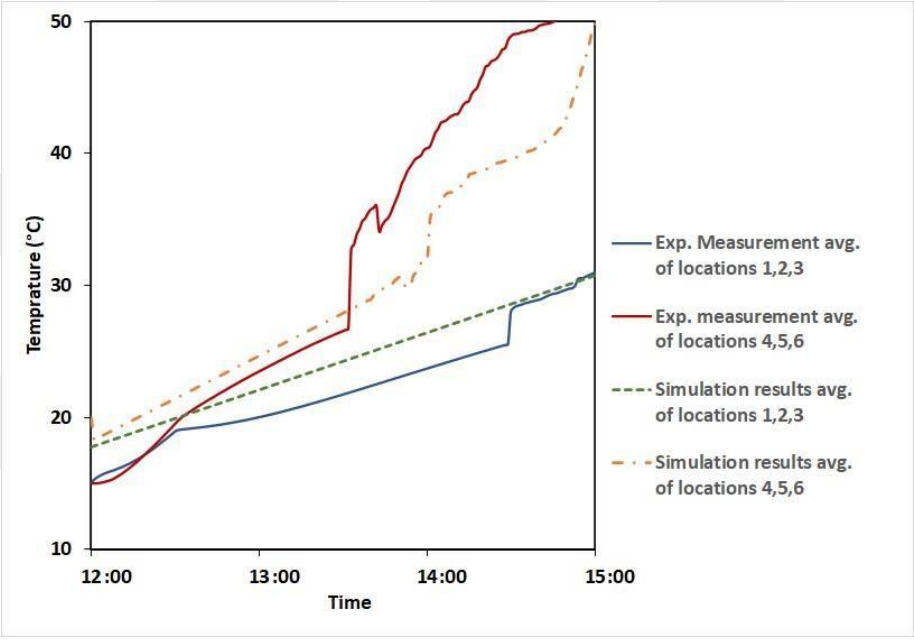

Figure 9 Comparison of the temperature values on the embedded thermocouples in PCMs between numerical and experimental results

Figure 9 compares the measured temperature from six embedded thermocouples in PCMs as shown in Fig. 4 and numerical simulation between 12:00 to 15:00 pm. It shows a good agreement in the average temperature of first three thermocouples, which measure the temperature of paraffin RRM_2 in the panel between the experimental measurement and numerical results. The maximum relative error is less than 12%. The average of second three thermocouples, which measure the temperature of paraffin RRM_1 in the panel, are in good agreement with the simulation results from 12:00 pm until 13:54 pm. After this time, however, the temperature difference and relative error rises about 9 °C and 18%, respectively.

There are many reasons why experimental and numerical results deviate. Inevitably, the measurement devices have an uncertainty range stated in Table 3. This error is not significant, but it needs to be considered in experimental studies. Installing measurement equipment into the test room affects the flow. Undoubtedly, it can be considered as an obstacle to the flow which will contribute to the deviation between experimental and numerical deviation. Another major discrepancy reason stems from the transient behavior of the experiments. For example, solar irradiation, ambient temperature, wind speed etc. vary during the day, but they are evaluated as a mean value for certain time periods. In numerical calculations, room walls are taken as insulated. In reality, there might be some heat gain to the room, especially when the forced convection (wind magnitude) is strong on both sides of the walls. It should be noted that PCM is assumed to be stagnant, and the only heat transfer mechanism in the PCM region is thermal conduction. Although the aspect ratio of the PCM contained is very high and PCM motion is very limited, this discrepancy needs to be evaluated. Besides, most of the thermophysical properties of the materials are taken as constant for a mean value. However, all temperatures vary due to the transient behavior of the experiment. Most importantly, the experimental setup is a scaled model of a real prison quarry. Hence, this dimensionality may affect the flow and heat transfer characteristics of the setup. In addition, dummy bodies are in cylindrical shape, and do not reflect the human body shapeexactly. Similarly, heat generation and the CO_2 release values of a person are the average values.

Figure 10 shows the specific locations of 26 sensors in the room model to measure the local temperature and CO_2 concentration. All sensors are positioned at the three basic levels (ground, mid-room, and roof level).

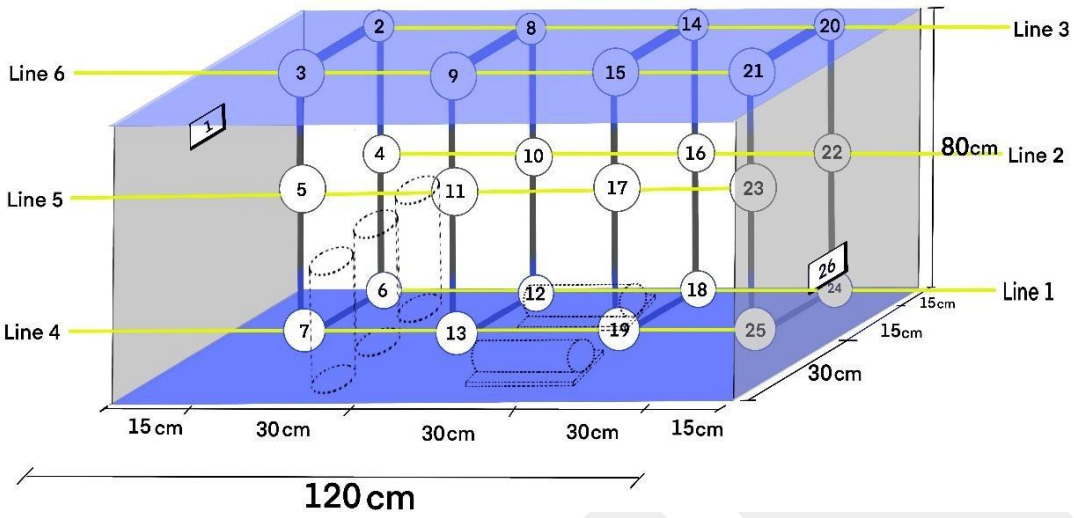

Figure 10 Position of sensors inside the scaled model

Instantaneous temperature values for each embedded sensors inside the room at inlet air velocity of 0.5 m/s are presented in Fig. 11. The results reveal that because of symmetrical geometry of the room at X direction, temperature values on lines 1, 2 and 3 are same as those on lines 4, 5 and 6, respectively. Besides, the experimental results are approximately overlapped with the theoretical ones for PCM usage case. The cooled air enters the room with temperature of 16 °C. Therefore, the temperature values on lines 3 and 6 for the sensors affected from the airflow are lower than those for the rest of the sensors. In addition, the temperature difference for two cases with and without PCM rises from the floor to the ceiling (lines 1,4 to lines 3,6). In other words, maximum temperature reductions by using PCM are about 6, 9, and 16 °C measured from sensors 18, 16, and 2, respectively. Consequently, applying PCM on the ceiling improves the thermal comfort of all occupants in the room.

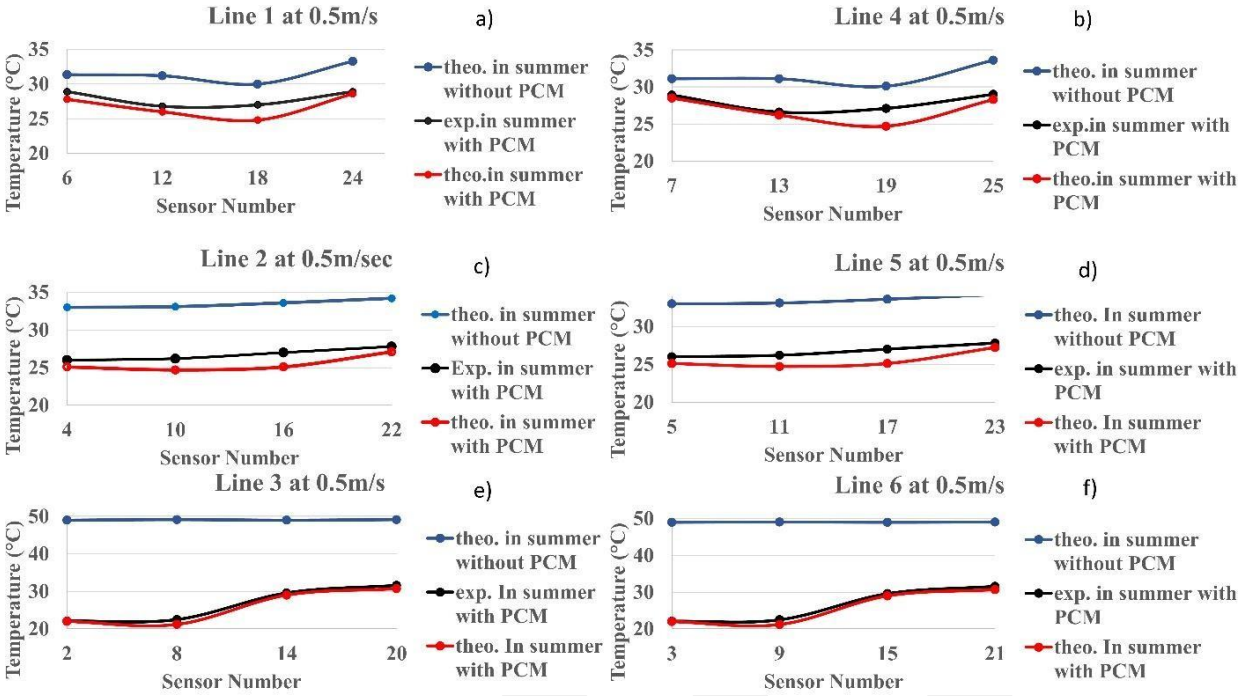

Figure 11 Temperature values measured by positioned sensors for inlet air velocity of 0.5 m/s, a) line 1, b) line 4, c) line 2, d) line 5, e) line 3, f) line 6

Figure 12 illustrates instantaneous carbon dioxide concentration values for each embedded sensors inside the room at an inlet air velocity of 0.5 m/s. The Numerical results and experimental measurements have matched well for all cases. Sensors record higher CO_2 concentrations for room without PCM than those with PCM on the floor. A significant CO_2 level reduction (more than 200 ppm) is observed on ground-level hypothetical lines (lines 1 and 4) by using PCM. No significant deviation exists for the mid-room (2-5) and roof level (3-6) lines. The carbon dioxide concentration with using PCM and without PCM do not exceed 570 ppm and 710 ppm, respectively during the computational time.

The threshold limit for indoor CO_2 is determined by ASHRAE as 1000 ppm. Although all the results are less than the acceptable threshold and pose no risk to the air-conditioned space, but applying PCM on the ceiling improves the comfort of all occupants in the room in terms of inhaling fresh air.

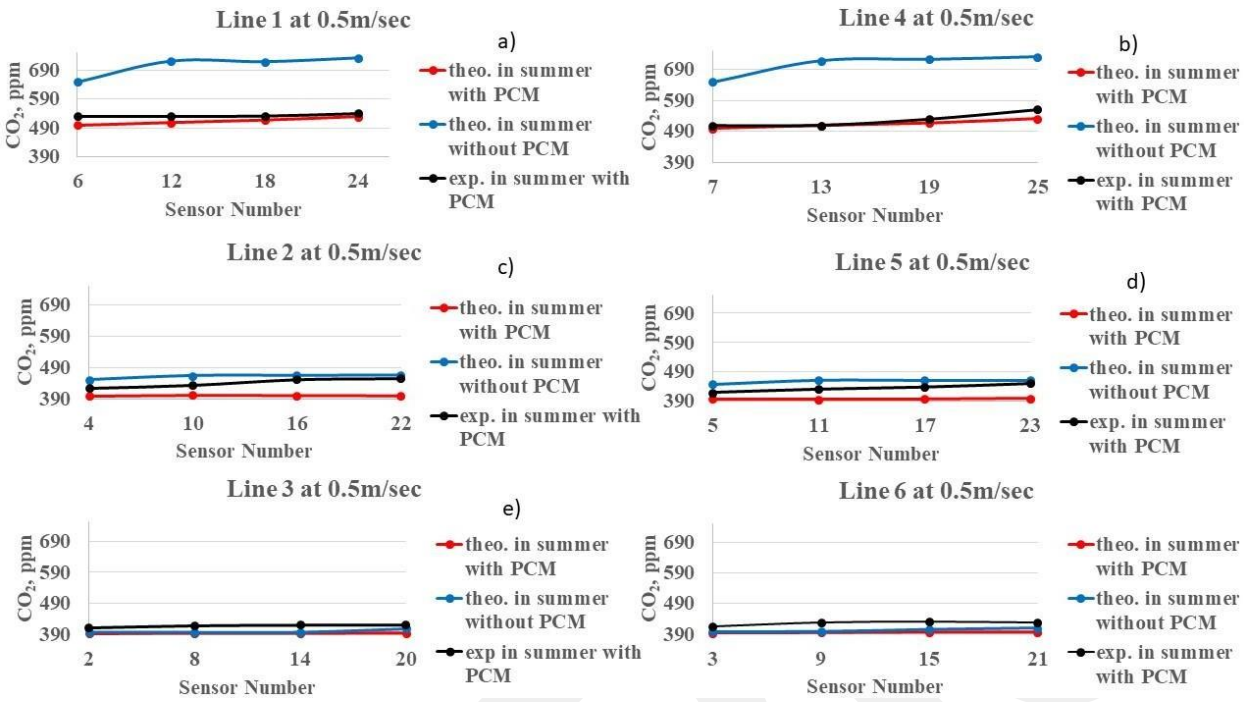

Figure 12 CO_2 concentration values measured by positioned sensors for inlet air velocity of 0.5 m/s, a) line 1, b) line 4, c) line 2, d) line 5, e) line 3, f) line 6

The power consumption during the cooling of the room with and without PCM is recorded during the day. The test was carried out on a typical summer day and the inlet air temperature and the thermostat set point are adjusted to 16°C and 26°C, respectively. Figure 13 demonestrates instantaneous power consumption by the air conditioner for cooling the test room at the air velocity of 0.5 m/s.

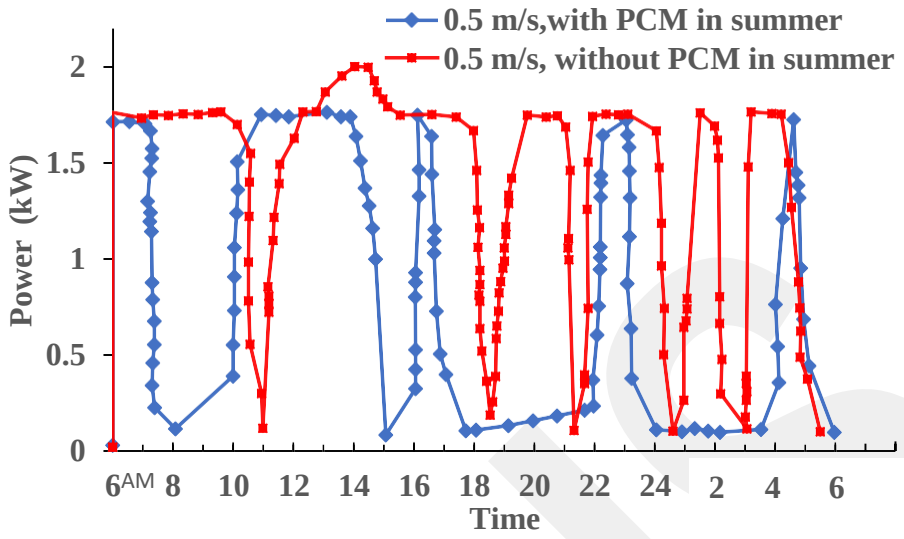

Figure 13 Experimental air conditioner power with and without PCM at inlet air velocity of 0.5m/s for one day in August.

The peak power of 2 kW is recorded for the room without PCM at 2 pm. The positive impact of PCM use is observed, especially between 5 pm to 6 am. The cooling system is not active for long hours, and the room temperature is below the set point temperature. The total energy consumption in 24 hours for the case without PCM is 29.5 kWh . However, this value reduces to 15.6 kWh for the room with PCM ceiling.

Figure 14 presents the instantaneous power of the air conditioner under the same conditions as the previous test, in which the inlet air velocity increases to 2.0 m/s. It can be seen that the compressor is working harder in the without PCM case, with three peak load zones. In contrast, the case with PCM operates without significant fluctuations.

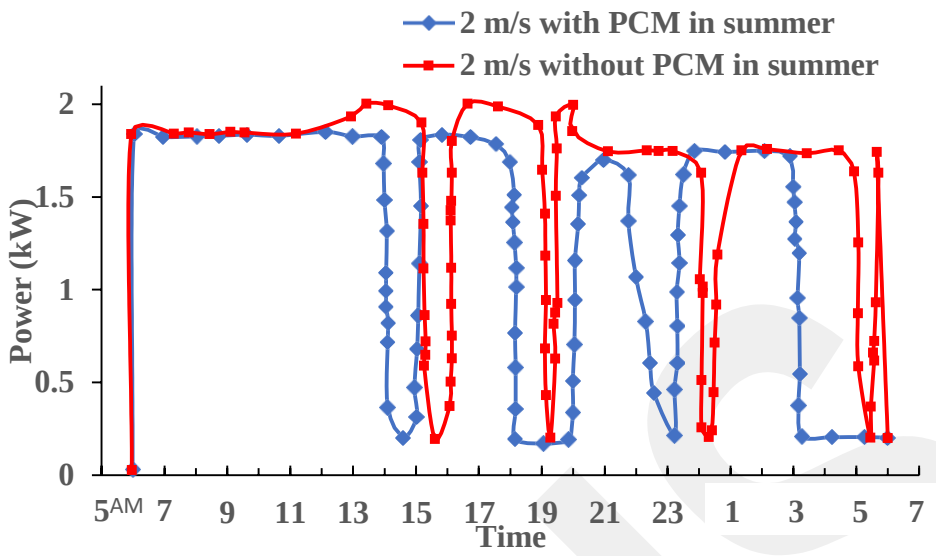

Figure 14 Experimental air conditioner power with and without PCM at inlet air velocity of 2 m/s for one day in August.

Figure 15 illustrates the experimental energy consumption in the cooling protocol with and without using PCM_s for different inlet air velocities.

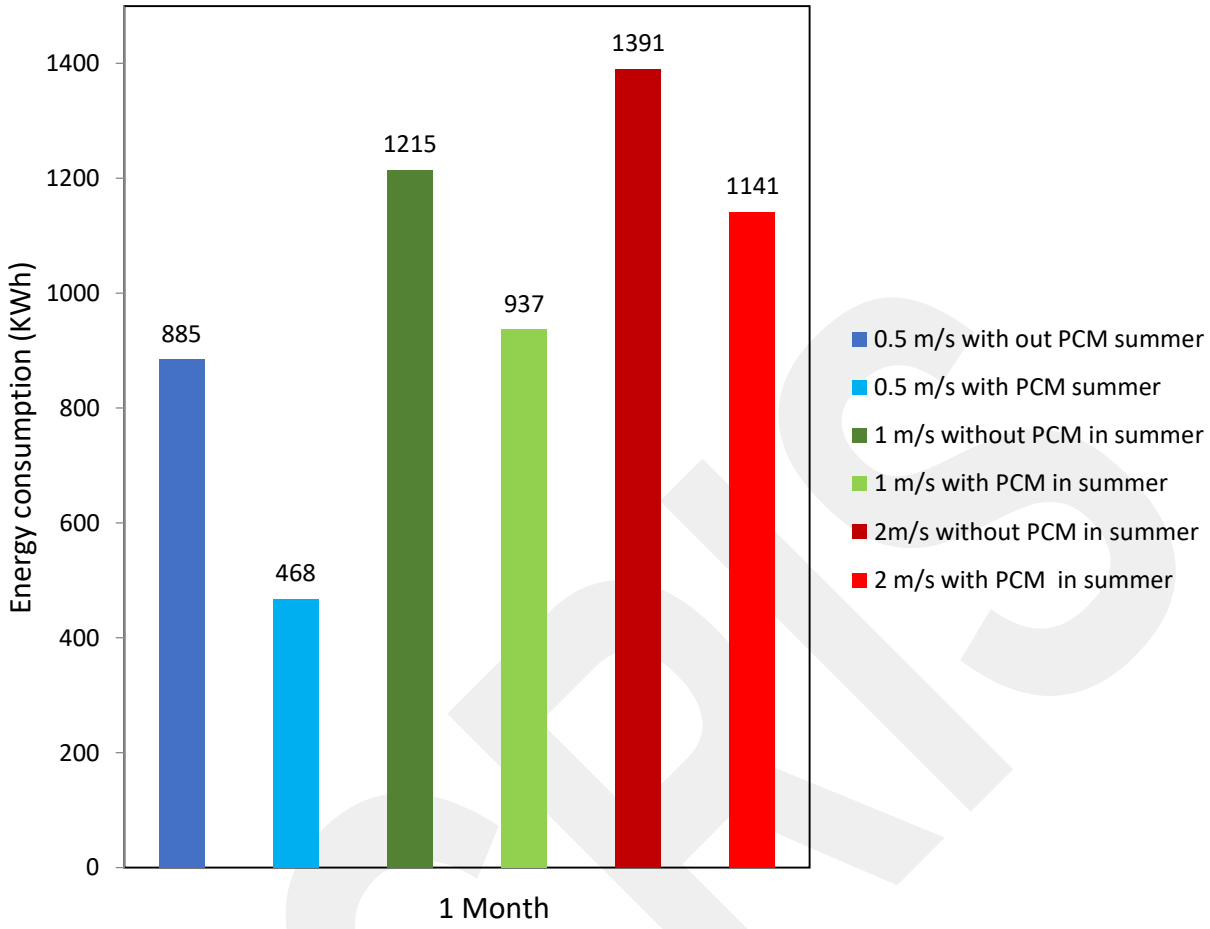

Figure 15 Monthly cooling energy consumption for the cases with and without PCM at inlet air velocities of 0.5, 1 and 2 m/s

It is clear that PCM has significantly reduced energy consumption, especially for the low inlet air velocity. It has a positive impact on the higher velocity cases as well, but not as much as the low velocity case. The energy savings using PCM is calculated as 47.2 %, 23% and 17.9% for inlet air velocities of 0.5 m/s, 1 m/s and 2 m/s, respectively. Considering electricity price of 0.12 USD/kWh for the first 5000 kWh consumption in Iraq, 50.1, 33.3, and 29.9 USD saving has been obtained with the PCM for the inlet air velocities of 0.5, 1, and 2 m/s, respectively.

4. Conclusion

The impact of PCM embedded in the room's ceiling has been examined. Experiments and numerical simulations have been conducted for severe summer conditions in Iraq. IAQ has been

evaluated in terms of temperature, water vapor, CO_2 concentration. Besides, the cooling energy consumption was calculated with and without PCM.

According to the experimental and numerical results, the following findings can be reported:

- Application of two layers of paraffin-based PCMs embedded in the ceiling, reduced the temperature at the center of the room by about 9 °C for the inlet air velocity of 0.5 m/s.
- Although carbon dioxide concentrations remained within safe levels for all cases, CO_2 concentration level were reduced by more than 200 ppm on the floor by using PCM.
- There was no considerable difference between the vapor volume fractions with and without PCM cases inside the room around the dummy bodies.
- A good agreement has been obtained between the experimental and numerical results.
- Using PCM reduced cooling energy consumption of the room by 47.2%, 23%, and 17.9% at inlet velocities of 0.5, 1, and 2 m/s, respectively.
- The results revealed that using PCM not only did improve IAQ in terms of temperature, carbon dioxide concentration, and humidity but also reduced the cooling energy consumption considerably.

The present study and most of the other studies in the literature have conducted transient simulations for a few hours, but cyclic (daily) analyses are needed to fully understand the phenomenon. Besides, experiments with real size quarry, and larger size human models under different seasonal and operational (number of people, activity level, etc.) conditions can be performed for more detailed analyses. Although PCM is isolated in a container, its effect on human health is an interdisciplinary research subject before conducting experiments with real human subjects. In line with the findings in the present study, a larger-scale analysis can be performed in terms of size and time. In addition, smart thermal control mechanisms can be developed for buildings equipped with PCM via methods like artificial intelligence, big data, and machine learning.

References

[1] Dincer I. On thermal energy storage systems and applications in buildings. n.d.

[2] Lu S, Gao J, Tong H, Yin S, Tang X, Jiang X. Model establishment and operation optimization of the casing PCM radiant floor heating system. Energy 2020;193. https://doi.org/10.1016/j.energy.2019.116814.

[3] Navarro L, de Gracia A, Colclough S, Browne M, McCormack SJ, Griffiths P, et al. Thermal energy storage in building integrated thermal systems: A review. Part 1. active storage systems. Renew Energy 2016;88:526–47. https://doi.org/10.1016/j.renene.2015.11.040.

[4] Belmonte JF, Eguía P, Molina AE, Almendros-Ibáñez JA. Thermal simulation and system optimization of a chilled ceiling coupled with a floor containing a phase change material (PCM). Sustain Cities Soc 2015;14:154–70. https://doi.org/10.1016/j.scs.2014.09.004.

[5] Koohi-Fayegh S, Rosen MA. A review of energy storage types, applications and recent developments. J Energy Storage 2020;27. https://doi.org/10.1016/j.est.2019.101047.

[6] Zhang C, Pomianowski M, Heiselberg PK, Yu T. A review of integrated radiant heating/cooling with ventilation systems- Thermal comfort and indoor air quality. Energy Build 2020;223. https://doi.org/10.1016/j.enbuild.2020.110094.

[7] Mousavi S, Rismanchi B, Brey S, Aye L. PCM embedded radiant chilled ceiling: A state-of-the-art review. Renewable and Sustainable Energy Reviews 2021;151. https://doi.org/10.1016/j.rser.2021.111601.

[8] Arıcı M, Bilgin F, Nižetić S, Karabay H. PCM integrated to external building walls: An optimization study on maximum activation of latent heat. Appl Therm Eng 2020;165. https://doi.org/10.1016/j.applthermaleng.2019.114560.

[9] Li D, Zheng Y, Liu C, Wu G. Numerical analysis on thermal performance of roof contained PCM of a single residential building. Energy Convers Manag 2015;100:147–56. https://doi.org/10.1016/j.enconman.2015.05.014.

[10] Adesina A. Use of phase change materials in concrete: current challenges. Renewable Energy and Environmental Sustainability 2019;4:9. https://doi.org/10.1051/rees/2019006.

[11] Alawadhi EM. Using phase change materials in window shutter to reduce the solar heat gain. Energy Build 2012;47:421–9. https://doi.org/10.1016/j.enbuild.2011.12.009.

[12] Solgi E, Hamedani Z, Fernando R, Mohammad Kari B. A parametric study of phase change material characteristics when coupled with thermal insulation for different Australian climatic zones. Build Environ 2019;163. https://doi.org/10.1016/j.buildenv.2019.106317.

[13] Kong X, Lu S, Huang J, Cai Z, Wei S. Experimental research on the use of phase change materials in perforated brick rooms for cooling storage. Energy Build 2013;62:597–604. https://doi.org/10.1016/j.enbuild.2013.03.048.

[14] Prabhakar M, Saffari M, de Gracia A, Cabeza LF. Improving the energy efficiency of passive PCM system using controlled natural ventilation. Energy Build 2020;228. https://doi.org/10.1016/j.enbuild.2020.110483.

[15] Al-Yasiri Q, Szabó M. Energetic and thermal comfort assessment of phase change material passively incorporated building envelope in severe hot Climate: An experimental study. Appl Energy 2022;314. https://doi.org/10.1016/j.apenergy.2022.118957.

[16] Al-Yasiri Q, Szabó M. Experimental study of PCM-enhanced building envelope towards energy-saving and decarbonisation in a severe hot climate. Energy Build 2023;279. https://doi.org/10.1016/j.enbuild.2022.112680.

[17] Al-Yasiri Q, Szabó M. Phase change material coupled building envelope for thermal comfort and energy-saving: Effect of natural night ventilation under hot climate. J Clean Prod 2022;365. https://doi.org/10.1016/j.jclepro.2022.132839.

[18] Gholamibozanjani G, Farid M. Experimental and mathematical modeling of an air-PCM heat exchanger operating under static and dynamic loads. Energy Build 2019;202. https://doi.org/10.1016/j.enbuild.2019.109354.

[19] Gholamibozanjani G, Farid M. A comparison between passive and active PCM systems applied to buildings. Renew Energy 2020;162:112–23. https://doi.org/10.1016/j.renene.2020.08.007.

[20] Bohórquez-Órdenes J, Tapia-Calderón A, Vasco DA, Estuardo-Flores O, Haddad AN. Methodology to reduce cooling energy consumption by incorporating PCM envelopes: A case study of a dwelling in Chile. Build Environ 2021;206. https://doi.org/10.1016/j.buildenv.2021.108373.

[21] Hagenau M, Jradi M. Dynamic modeling and performance evaluation of building envelope enhanced with phase change material under Danish conditions. J Energy Storage 2020;30. https://doi.org/10.1016/j.est.2020.101536.

[22] Ma L, Luo D, Hu H, Li Q, Yang R, Zhang S, et al. Energy performance of a rural residential building with PCM-silica aerogel sunspace in severe cold regions. Energy Build 2023;280. https://doi.org/10.1016/j.enbuild.2022.112719.

[23] Yang S, Zhang Y, Zhao Y, Torres JF, Wang X. PCM-based ceiling panels for passive cooling in buildings: A CFD modelling. Energy Build 2023;285. https://doi.org/10.1016/j.enbuild.2023.112898.

[24] Rangel CG, Rivera-Solorio CI, Gijón-Rivera M, Mousavi S. The effect on thermal comfort and heat transfer in naturally ventilated roofs with PCM in a semi-arid climate: An experimental research. Energy Build 2022;274. https://doi.org/10.1016/j.enbuild.2022.112453.

[25] Németh B, Ujhidy A, Tóth J, Ferencz M, Kurdi R, Gyenis J, et al. Power consumption of model houses with and without PCM plaster lining using different heating methods. Energy Build 2023;284. https://doi.org/10.1016/j.enbuild.2023.112845

[26] Mousavi, S., Rismanchi, B., Brey, S., & Aye, L. (2021). PCM embedded radiant chilled ceiling: A state-of-the-art review. In *Renewable and Sustainable Energy Reviews* (Vol. 151). Elsevier Ltd. https://doi.org/10.1016/j.rser.2021.111601

[27] Alassaad, F., Touati, K., Levacher, D., & Sebaibi, N. (2023). Effect of latent heat storage on thermal comfort and energy consumption in lightweight earth-based housings. *Building and Environment*, *229*. https://doi.org/10.1016/j.buildenv.2022.109915

[28] Zhu, X., Sheng, X., Li, J., & Chen, Y. (2021). Thermal comfort and energy saving of novel heat-storage coatings with microencapsulated PCM and their application. *Energy and Buildings*, *251*. https://doi.org/10.1016/j.enbuild.2021.111349

[29] Berardi, U., & Soudian, S. (2019). Experimental investigation of latent heat thermal energy storage using PCMs with different melting temperatures for building retrofit. *Energy and Buildings*, *185*, 180–195. https://doi.org/10.1016/j.enbuild.2018.12.016

[30] Kheradmand, M., Azenha, M., de Aguiar, J. L. B., & Castro-Gomes, J. (2016). Experimental and numerical studies of hybrid PCM embedded in plastering mortar for enhanced thermal behaviour of buildings. *Energy*, *94*, 250–261. https://doi.org/10.1016/j.energy.2015.10.131

[31] Favoino, F., Goia, F., Perino, M., & Serra, V. (2014). Experimental assessment of the energy performance of an advanced responsive multifunctional façade module. *Energy and Buildings*, *68*(PART B), 647–659. https://doi.org/10.1016/j.enbuild.2013.08.066

[32] Guarino, F., Athienitis, A., Cellura, M., & Bastien, D. (2017). PCM thermal storage design in buildings: Experimental studies and applications to solaria in cold climates. *Applied Energy*, *185*, 95–106. https://doi.org/10.1016/j.apenergy.2016.10.046

[33] Entrop, A. G., Brouwers, H. J. H., & Reinders, A. H. M. E. (2011). Experimental research on the use of micro-encapsulated Phase Change Materials to store solar energy in concrete floors and to save energy in Dutch houses. *Solar Energy*, *85*(5), 1007–1020. https://doi.org/10.1016/j.solener.2011.02.017

[34] Elnour, M., Himeur, Y., Fadli, F., Mohammedsherif, H., Meskin, N., Ahmad, A. M., Petri, I., Rezgui, Y., & Hodorog, A. (2022). Neural network-based model predictive control system for optimizing building automation and management systems of sports facilities. *Applied Energy*, *318*. https://doi.org/10.1016/j.apenergy.2022.119153

[35] Himeur, Y., Elnour, M., Fadli, F., Meskin, N., Petri, I., Rezgui, Y., Bensaali, F., & Amira, A. (2023). AI-big data analytics for building automation and management systems: a survey, actual challenges and future perspectives. *Artificial Intelligence Review*, *56*(6), 4929–5021. https://doi.org/10.1007/s10462-022-10286-2

[36] Himeur, Y., Ghanem, K., Alsalemi, A., Bensaali, F., & Amira, A. (2021). Artificial intelligence based anomaly detection of energy consumption in buildings: A review, current trends and new perspectives. In *Applied Energy* (Vol. 287). Elsevier Ltd. https://doi.org/10.1016/j.apenergy.2021.116601

[37] Elnour, M., Fadli, F., Himeur, Y., Petri, I., Rezgui, Y., Meskin, N., & Ahmad, A. M. (2022). Performance and energy optimization of building automation and management systems: Towards smart sustainable carbon-neutral sports facilities. In *Renewable and Sustainable Energy Reviews* (Vol. 162). Elsevier Ltd. https://doi.org/10.1016/j.rser.2022.112401

[38] Himeur, Y., Elnour, M., Fadli, F., Meskin, N., Petri, I., Rezgui, Y., Bensaali, F., & Amira, A. (2022). Next-generation energy systems for sustainable smart cities: Roles of transfer learning. In *Sustainable Cities and Society* (Vol. 85). Elsevier Ltd. https://doi.org/10.1016/j.scs.2022.104059

[39] Mohammed FA, Al-Malaki K. EXPERIMENTAL EVALUATION AND CFD STUDY OF THERMAL COMFORT, IAQ INDICES, AND THERMAL ENERGY STORAGE FOR THE IMPROVEMENT OF THE ENERGY PERFORMANCE OF OVERCROWDED AREA THE GRADUATE SCHOOL OF NATURAL AND APPLIED SCIENCES OF ATILIM UNIVERSITY DOCTOR OF PHILOSOPHY THESIS IN THE DEPARTMENT OF MODELING AND

DESIGN OF ENGINEERING SYSTEMS (MAIN FIELD OF STUDY: MECHANICAL ENGINEERING). n.d.

[40] Al-Malaki F, Jafari R. Numerical Evaluation of Thermal Comfort, IAQ Indices, and TES for the Improvement of the Energy Performance in Crowded Area. IICETA 2022 - 5th International Conference on Engineering Technology and its Applications, Institute of Electrical and Electronics Engineers Inc.; 2022, p. 6–13. https://doi.org/10.1109/IICETA54559.2022.9888615.

[41] Thermal Environmental Conditions for Human Occupancy 2004.

[42] Türkakar G. Thermal Analysis and Parametric Investigation of Phase Change Material-Air Cooled Lithium Ion Battery Pack. J Heat Transfer 2021;143. https://doi.org/10.1115/1.4052154.

[43] Kothari R, Das S, Sahu SK, Kundalwal SI. Analysis of solidification in a finite PCM storage with internal fins by employing heat balance integral method. Int J Energy Res 2019;43:6366–88. https://doi.org/10.1002/er.4363.

Declaration of interests

☒The authors declare that they have no known competing financial interests or personal relationships that could have appeared to influence the work reported in this paper.

☐The authors declare the following financial interests/personal relationships which may be considered as potential competing interests: